



OPEN

Antifreeze protein from *Ammopiptanthus nanus* functions in temperature-stress through domain A

HaoQiang Yu¹, HongYing Zheng¹, Yuan Liu¹, QingQing Yang¹, WanChen Li¹, YuanYuan Zhang²✉ & FengLing Fu¹✉

Temperature stress restricts plant growth and development. Antifreeze protein (AFP) can improve plants antifreeze ability. In our previous study, the *AnAFP* gene cloned from *Ammopiptanthus nanus* was confirmed to be an excellent candidate enhancing plant cold resistance. But, AnAFP protein shared similar structures with KnS type dehydrins including K, N and S domains except ice crystal binding domain A. Here, we generated *AnAFPΔA*, *AnAFPΔK*, *AnAFPΔN* and *AnAFPΔS*, and transformed them into ordinary and cold sensitive strains of *E. coli*, and *Arabidopsis* KS type dehydrin mutant to evaluate their function. Expression of *AnAFPΔA* decreases cold and heat tolerance in *E. coli*, meanwhile, AnAFP enhances heat tolerance in *Arabidopsis*, suggesting that domain A is a thermal stable functional domain. AnAFP, *AnAFPΔA* and *AnAFPΔS* localize in whole cell, but *AnAFPΔK* and *AnAFPΔN* only localizes in nucleus and cytoplasm, respectively, exhibiting that K and N domains control localization of AnAFP. Likewise, K domain blocks interaction between AnAFP and AnICE1. The result of RT-qPCR showed that expression of *AnAFP*, *AnICE1* and *AnCBF* genes was significantly induced by high-temperature, indicating that the *AnAFP* is likely regulated by ICE1-CBF-COR signal pathway. Taken together, the study provides insights into understanding the mechanism of AnAFP in response to temperature stress and gene resource to improve heat or cold tolerance of plants in transgenic engineering.

Temperature stress including low- and high-temperature stress restricts plant growth and development. Low temperature inhibits enzyme activity and destroys membrane permeability resulting in physiological disorder, metabolic obstruction and even cell death^{1,2}. Similarly, high temperature leads to wilting, accumulation of reactive oxygen species (ROS), and destruction of membrane system³⁻⁵. After perceiving temperature stress, plants approach genes expression change, physiological and biochemical response via signal transduction⁵⁻⁸. The ICE1-CBF-COR pathway is the most studied signaling pathway under temperature stress in plants. Under low temperature conditions, a MYC-like basic helix loop helix (bHLH) transcription factor ICE1 (Inducer of CBF expression 1) induces expression of the CBF gene. The CBF transcription factor binds to the CRT/DRE (C-repeats/dehydration responsive) element (CCGAC) and activates the expression of cold-responsive genes (COR)^{9,10}. In response to high temperature stress, the energy releasing from cell physiological disorder such as membrane fluidity increasing, DNA unwinding and protein subunit dissociation triggers transcriptional changes to restore homeostasis, promoting cell survival, and elaborating longer-term responses for adaptation, growth, and development¹¹.

Antifreeze proteins (AFPs) were firstly found in polar fishes, as well as insects living in freeze-zone. AFPs prevent water from freezing by adsorbing to the ice surface and stopping the growth of minute ice crystals to large crystals in a non-colligative manner, and help the organisms survive in subzero temperature environments. The distribution of AFPs in different species appears to be the outcome of a combination of independent evolutionary events, which is probably the convergent evolution or horizontal gene transfer¹². These AFPs genes were introduced into crops to improve their tolerance to low temperature stress. Expression of antifreeze protein of winter flounder or insect (*Microdera puntipennis dzungarica*) confers the cold tolerance to transgenic spring

¹Key Laboratory of Biology and Genetic Improvement of Maize in Southwest Region, Ministry of Agriculture; Maize Research Institute, Sichuan Agricultural University, Chengdu 611130, China. ²College of Life Science & Biotechnology, Mianyang Teachers' College, Mianyang 621000, China. ✉email: 199774@mnu.cn; ffl@sicau.edu.cn

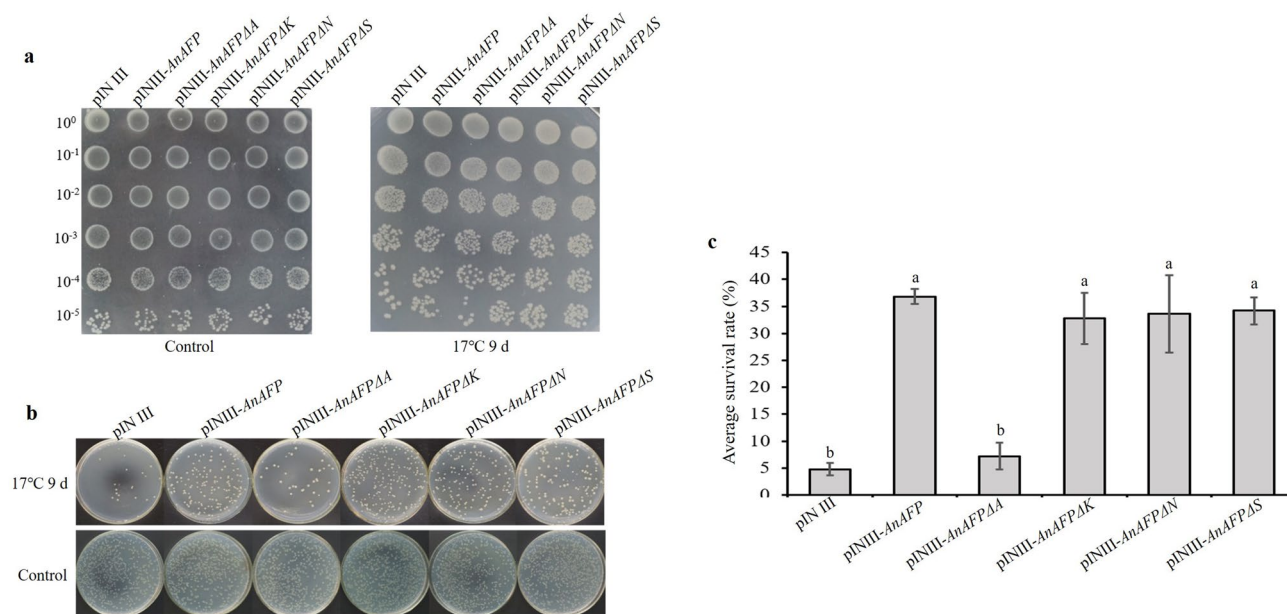


Figure 1. Phenotype of cold sensitive BX40 strain of *E. coli* with *AnAFP*, *AnAFPΔA*, *AnAFPΔK*, *AnAFPΔN* and *AnAFPΔS* gene under low temperature stress (17 °C) for 9 days. **(a)** Colony growth of different dilution times. **(b)** Monoculture of transformed strains. **(c)** Average survival rate of transformed strains. Lower case letter indicates the significant difference at $p < 0.05$ level in student's *t*-test. The experiment was performed with three replicates. The data were presented as the mean values \pm SD.

wheat at subzero temperatures, tobacco or tomato, respectively^{13–15}. Meanwhile, the transgenic plants did not demonstrate significant tolerance improvement when compared to wild-types^{13–15}. The non-colligative manner of the heterologous animal AFPs, as well as their expression rate, localization, and stability, might not be suitable for cellular environments in transgenic plants¹⁶. However, the AFPs from overwintering plants including *Lolium perenne*, *Lolium perenne* and *Ammopiptanthus nanus* showed higher inhibitory effect on ice growth and recrystallization than that of AFPs of fishes and insects^{17–20}.

Ammopiptanthus nanus (*A. nanus*) is a tertiary relict plant and evergreen broad-leaved shrub distributed in deserts in Central Asia, exhibits excellent tolerance to abiotic stress including drought, low and high temperature. In our previous study, the *AnAFP* gene was cloned from xerophyte *A. nanus*, and evaluated its cold tolerance function by ectopic expression in *Escherichia coli* (*E. coli*), tobacco and maize^{21,22}. Bioinformatics analysis showed that *AnAFP* shared high similarity with some members of KnS type dehydrins²². In addition to the ice crystal binding domain (A domain) of AFPs, *AnAFP* also has three conserved domains of dehydrins including K, S and N (Nuclear localization sequence) domains^{22,23}. In order to evaluate the function of these domains, four mutants of *AnAFP* deleting A (*AnAFPΔA*), K (*AnAFPΔK*), S (*AnAFPΔS*) and N (*AnAFPΔN*) domain were generated by overlapping PCR, respectively. In this study, these four mutants and *AnAFP* were introduced into cold-sensitive and ordinary strains of *E. coli*, as well as *Arabidopsis* mutant of KnS type dehydrin gene *AtHIRD11* to identify thermal stability of each domain under low- and high-temperature stress, respectively. Together with their sub-cellular localization, interacting proteins and induced endogenous expression, the regulation mechanism of the *AnAFP* protein in response to temperature stress was elucidated.

Results

Sequence of mutant genes. Through overlap PCR, the sequences of *AnAFPΔA*, *AnAFPΔK*, *AnAFPΔN* and *AnAFPΔS* were amplified from *AnAFP* (Figure S1a). Their encoding putative proteins were deleted of crystal binding domain A, and K, NLS and S domains of dehydrin, respectively (Figure S1b).

Expression of *AnAFPΔA* increases cold sensitivity of BX04. After low temperature treatment at 17 °C for 9 days, the cold-sensitive BX04 containing pINIII-*AnAFPΔA* showed growth defect and failed to form colonies with an average survival rate $< 10\%$, which was similar to BX04 cells contain pINIII. However, the BX04 containing pINIII-*AnAFPΔK*, pINIII-*AnAFPΔS* and pINIII-*AnAFPΔN* grew vigorously and formed more colonies with an average survival rate $> 30\%$, respectively, which was similar to BX04 cells with pINIII-*AnAFP* (Fig. 1). These results suggest that domain A is a functional domain of *AnAFP* protein related to cold tolerance.

Expression of *AnAFPΔA* increases heat sensitivity of BL21. After IPTG induction, the expression of candidate genes in BL21 was confirmed and analyzed by SDS-PAGE (Figure S2). After 30 min of heat treatment at 50 °C, the colony growth of each dilution time of the *E. coli* BL21 transformed by pET28a was inhibited, and the average survival rate was only 14.46%. Whereas the BL21 cells with pET28a-*AnAFP* grew better, with an average survival rate of 85.29%. Notably, the BL21 cells with pET28a-*AnAFPΔA* was similar to BL21 with pET28a,

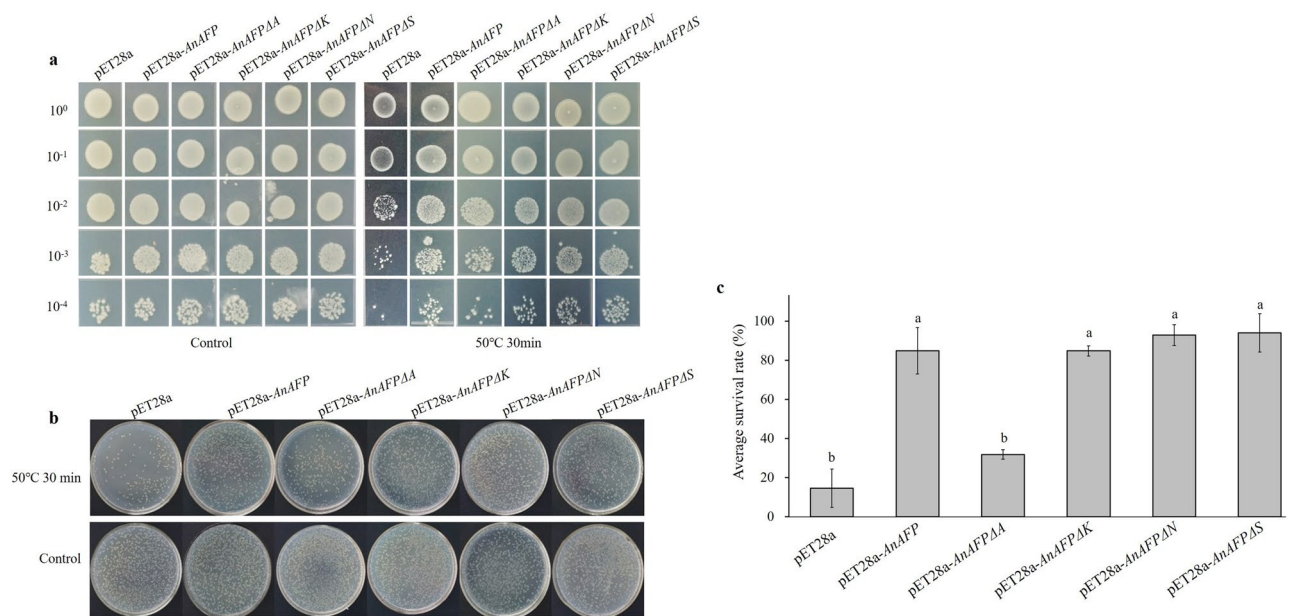


Figure 2. Thermotolerant phenotype of *E. coli* BL21 strains transformed by *AnAFP*, *AnAFPΔA*, *AnAFPΔK*, *AnAFPΔN* and *AnAFPΔS* gene under heat stress (50 °C) for 30 min. **(a)** Colony growth of different dilution times. **(b)** Monoclonal growth of transformed strains. **(c)** Average survival rate. Lower case letter indicates the significant difference at $p < 0.05$ level in student's *t*-test. The experiment was performed with three replicates. The data were presented as the mean values \pm SD.

the average survival was 32.41%. However, the BL21 cells with pET28a-*AnAFPΔK*, pET28a-*AnAFPΔN*, and pET28a-*AnAFPΔS* was similar to that transformed by pET28a-*AnAFP*, and average survival rates were 84.85%, 95.75% and 95.85%, respectively (Figs. 2 and S3), suggesting that A domain as ice crystal binding domain was also related to thermostable function of AnAFP protein.

Expression of mutant genes increase heat sensitivity of *Arabidopsis*. After screening with 50 mg/L kanamycin, the five homozygous lines for every gene were identified by PCR amplification of *AnAFPΔA*, *AnAFPΔK*, *AnAFPΔN* and *AnAFPΔS*, respectively (Figure S4), indicating that these genes were integrated into the genome of *Arabidopsis*. Subsequently, the ORF of *AnAFPΔA*, *AnAFPΔK*, *AnAFPΔN* and *AnAFPΔS* were amplified by RT-PCR from the T₃ lines of transgenic lines, but not in untransformed mutant. Likewise, the specific fragment of *AtActin* was amplified both in transgenic lines and untransformed mutant (Figs. 3 and S5), indicating the ectopic expression of candidate genes in transgenic plants.

As shown in Fig. 4, before heat treatment, the transgenic lines and untransformed mutants grew vigorously. After 46 °C treatment for 3 h and then recovered 2 weeks, the transgenic lines transformed by *AnAFPΔA*, *AnAFPΔK*, *AnAFPΔN* and *AnAFPΔS* and untransformed mutants all died. However, a few plants of transgenic line transformed by *AnAFP* still survived. This result suggests that ectopic expression of *AnAFP* improves heat tolerance of heat sensitive *Arabidopsis* mutant. However, deletion of any one of A, K, N and S domains will lead to loss of heat resistance function of AnAFP protein.

Deletion of domains K and N alters subcellular localization. Subcellular localization results showed that green fluorescence signals were observed both in cytoplasm and nucleus of onion epidermal cells transformed by 35S-*eGFP*, 35S-*AnAFP-eGFP*, 35S-*AnAFPΔA-eGFP*, and 35S-*AnAFPΔS-eGFP*, respectively. However, green fluorescence was observed only in the nucleus of onion epidermal cells with 35S-*AnAFPΔK-eGFP*, and only in the cytoplasm of onion epidermal cells with 35S-*AnAFPΔN-eGFP* (Fig. 5). These results suggest that the deletion of domains K and N changes the subcellular localization of AnAFP protein.

Domain K blocks interaction of AnAFP with AnICE1. As shown in Fig. 6, the yeast Y2H Gold co-transformed by bait vector and trap vector could grow normally on SD/-Leu-Trp plates, but not grow and not turn blue on SD/-Leu-Trp-His-Ade with X- α -Gal plates except positive control (pGADT7-T + pGBKT7-53), showing that these proteins have no toxicity and no autoactivation in yeast cell. Likewise, the yeast cells with pGBKT7-*AnAFPΔK* and pGADT7-*AnICE1* could grow and be stained to blue on the auxotroph SD/-Leu-Trp-His-Ade with X- α -gal plates, while the cells co-transformed by pGBKT7-*AnAFP*, pGBKT7-*AnAFPΔA*, pGBKT7-*AnAFPΔN*, pGBKT7-*AnAFPΔS*, and pGADT7-*AnICE1* did not grow, suggesting that AnAFPΔK interacts with AnICE1. This result indicates that domain K of AnAFP protein blocks its interaction with AnICE1 protein.

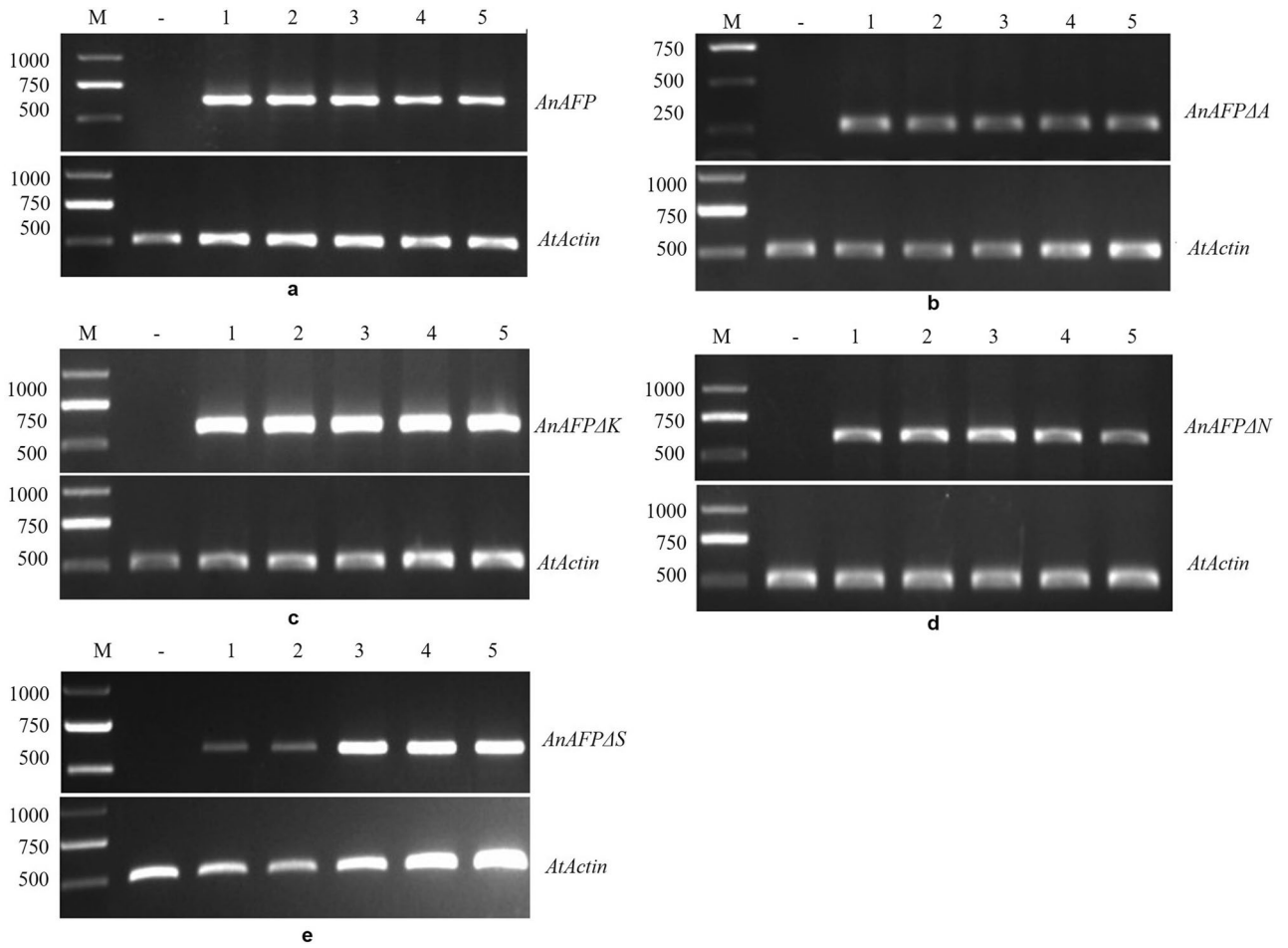


Figure 3. Ectopic expression of *AnAFP* (a), *AnAFPΔA* (b), *AnAFPΔK* (c), *AnAFPΔN* (d), *AnAFPΔS* (e) genes in T_3 transgenic *Arabidopsis* by RT-PCR. M: DNA molecular weight marker DL2000; -: Untransformed mutant; 1, 2, 3, 4, 5 indicates independent transgenic line.

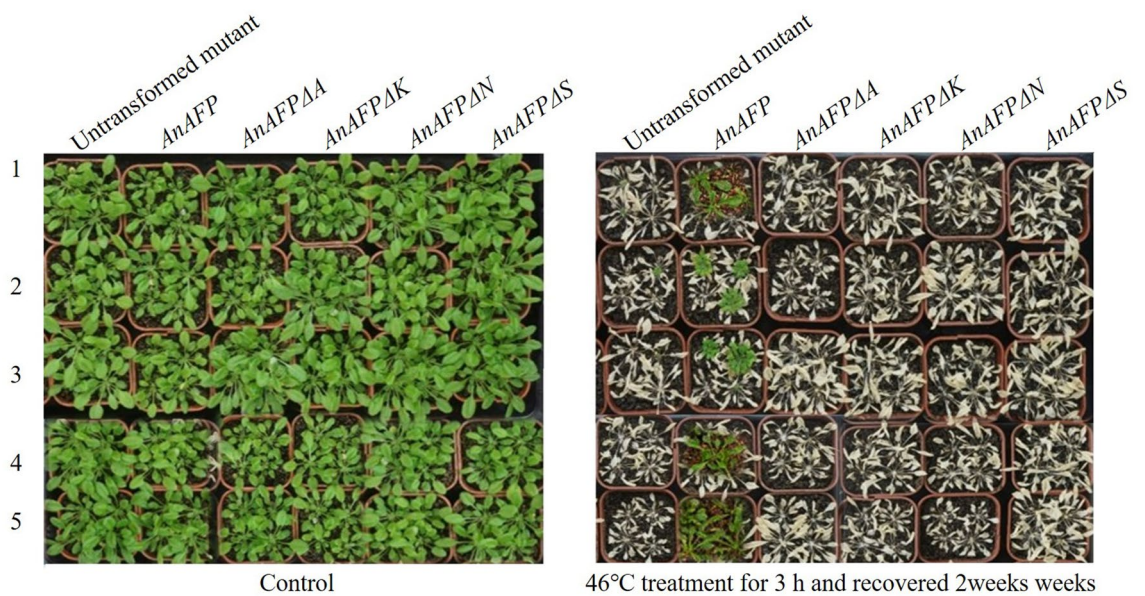


Figure 4. Phenotype of T_3 transgenic lines and untransformed mutant under heat treatment. 1, 2, 3, 4, 5 indicates independent transgenic line. Five T_3 lines were planted in pots, and grown in green house at 22 °C and 60–70% relative humidity under a 10 h light/14 h dark photoperiod. One-month-old seedlings were used for heat-shock treatment at 46 °C for 3 h, and recovered for 2 weeks at 22 °C, and investigated for phenotype.

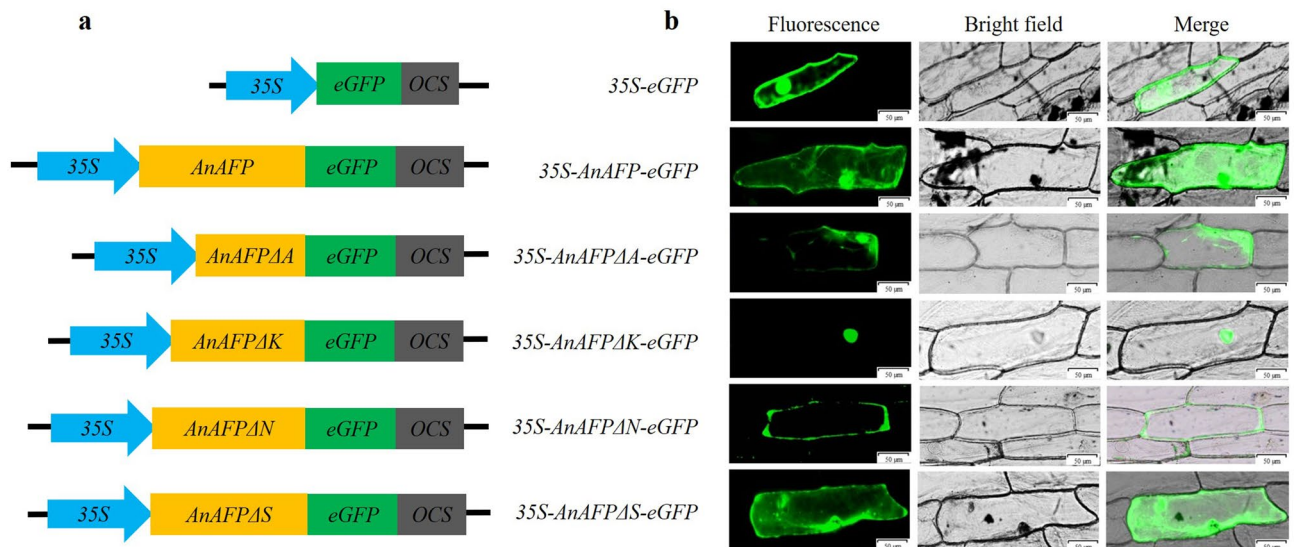


Figure 5. Subcellular localization of AnAFP and its deletion mutants in onion epidermal cells. **(a)** The diagram of vector for transient expression. **(b)** Green fluorescence observed by confocal microscopy. Scale bars = 50 μm.

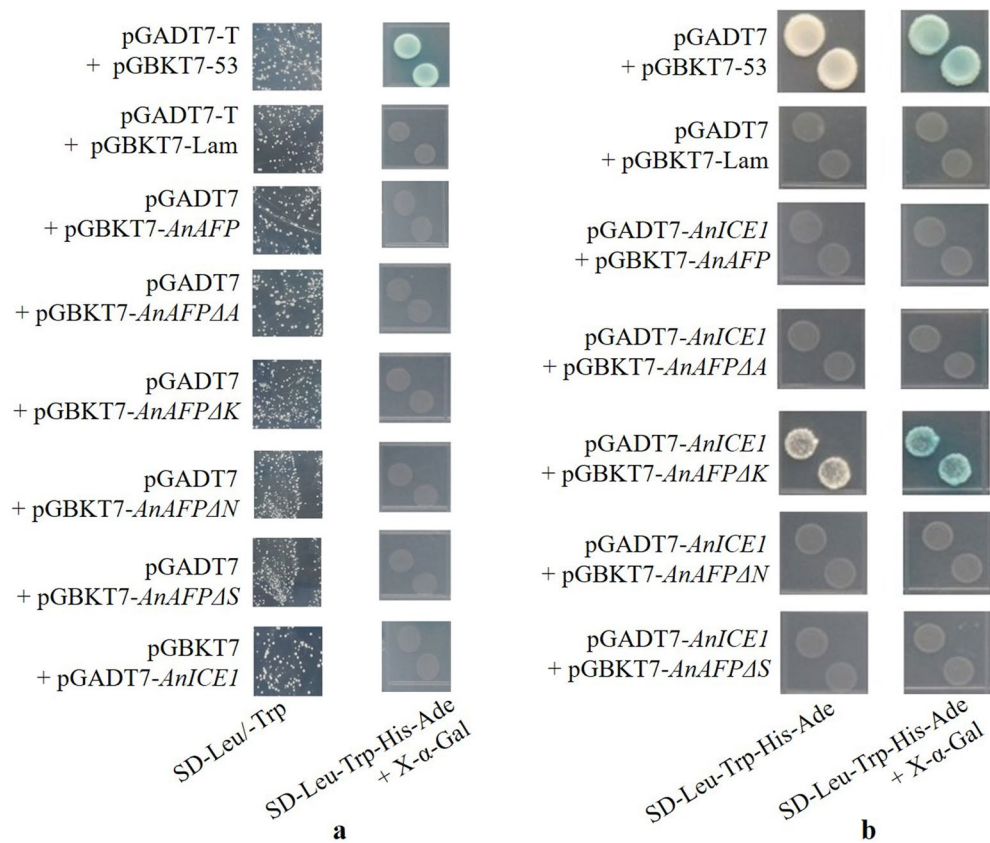


Figure 6. Protein interaction by Y2H. **(a)** The toxicity and autoactivation assay. **(b)** Y2H between AnICE1 and AnAFP, as well as its deletion mutants.

Endogenous expression of *AnAFP*, *AnICE1* and *AnCBF* genes in response to high temperature stress. The results of real-time quantitative PCR (RT-qPCR) showed that the expression of *AnAFP*, *AnICE1* and *AnCBF* genes were significantly upregulated by high temperature stress. The expression of *AnAFP* reached to 13.91 times of control at 6 h of treatment. Meanwhile, at 3 h of treatment, the expression of *AnICE1* and *AnCBF* increased to 2.86 and 18.50 times of control (0 h), respectively (Fig. 7). This result suggests that the

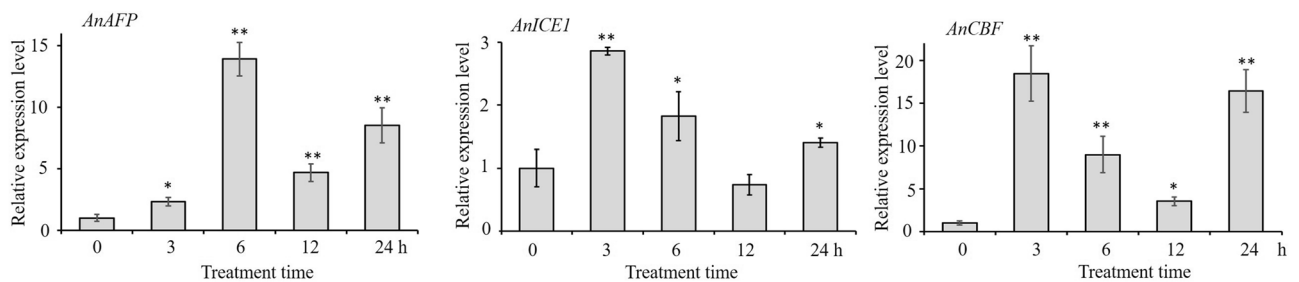


Figure 7. Relative expression levels of *AnAFP*, *AnICE1* and *AnCBF* genes under high temperature (45 °C) treatment. The *AnGAPDH* gene was used as internal reference. The $2^{-\Delta\Delta CT}$ method of the CFX Manger™ software version 2.0 (Bio-Rad, USA) was used to normalize the expression differentiation between reference gene and investigated genes. The experiment was performed with three replicates. The data were presented as the mean values \pm SD.

upregulated expression of *AnAFP* gene in response to high temperature stress maybe regulated by the signaling pathway of ICE1-CBF-COR.

Discussion

All AFPs are conserved for their ice crystal binding sites, although difference in their structural characteristics due to their different evolution^{24,25}. Under low temperature stress (17 °C for 9 days), the colony growth and average survival rates of the cold-sensitive *E. coli* BX04 with *AnAFP* Δ A were significantly poorer and lower than the strains transformed with *AnAFP*, as well as *AnAFP* Δ K, *AnAFP* Δ N and *AnAFP* Δ S mutants (Fig. 1). Under high temperature stress (50 °C for 30 min), the colony growth and average survival rate of *E. coli* BL21 (DE3) transformed by *AnAFP* Δ A were also significantly poorer and lower than the strains transformed by *AnAFP*, as well as *AnAFP* Δ K, *AnAFP* Δ N and *AnAFP* Δ S (Fig. 2). These results confirmed the conserved thermostable function of ice crystal binding domain (domain A) in *AnAFP* proteins. However, the function of each domain of *AnAFP* is not indispensable. All T₃ plants of *Arabidopsis* mutant of KnS type dehydrin *athird11* transformed by *AnAFP* Δ A, *AnAFP* Δ K, *AnAFP* Δ N and *AnAFP* Δ S mutants died after high temperature stress (46 °C for 3 h), while a few T₃ plants of the same mutant transformed by the *AnAFP* gene survived (Fig. 4). Subcellular localization showed that the mutants without domains A and S were localized in the cytoplasm and nucleus, which was same as *AnAFP* protein. However, the mutant without domain K was only localized in the nucleus, while the mutant without domain N was localized only in the cytoplasm (Fig. 5). This result suggests that domains K and N determine the subcellular localization of *AnAFP* protein and affect its function. Similar phenomenon was observed for KnS-type dehydrin ZmDHN13 in maize²⁶.

The Y2H result indicates that domain K of *AnAFP* protein blocks its interaction with *AnICE1* proteins (Fig. 6). This result can be explained by the molecular shield model of dehydrin to protect functional proteins^{27,28}. The internal disordered structure of dehydrin protein occupies the space between the target proteins and reduces their collision. This kind of shield forms a loose structure around the target protein but not interact with it like the classical molecular chaperone.

In our previous study, the *AnAFP* was found to be a KnS type dehydrin and the *AnAFP* gene was identified as a member of *COR* genes²². Dehydrin and *COR* genes can be activated by CBF participating ICE1-CBF-COR pathway^{29–32}. In the present study, the RT-qPCR result showed that the endogenous expression of *AnAFP*, *AnICE1* and *AnCBF* genes was significantly upregulated by high temperature stress (Fig. 7). It suggests that high temperature stress also induces the expression of *COR* genes. In response to low and high temperature stress, the endogenous expression of *AnAFP* is probably induced by signaling pathway of ICE1-CBF-COR. In *Arabidopsis*, the expression of heat shock proteins was also found to be extensively overlapped with non-heat stress response pathways³³. Therefore, the regulation of the endogenous expression of *AnAFP* in *A. nanus* can be concluded as signaling pathway sketched in Fig. 8.

Conclusion

In the presents study, we generated *AnAFP* Δ A, *AnAFP* Δ K, *AnAFP* Δ N and *AnAFP* Δ S, and transformed them into ordinary and cold sensitive strains of *E. coli*, and *Arabidopsis* KS type dehydrin mutant to evaluate their function. It's confirmed that domain A is a thermal stable functional domain, K and N domains control localization of *AnAFP*. Likewise, K domain blocks interaction between *AnAFP* and *AnICE1*. The expression of *AnAFP*, *AnICE1* and *AnCBF* genes was significantly induced by high-temperature, indicating that the *AnAFP* is likely regulated by ICE1-CBF-COR signal pathway.

Materials and methods

Evaluation of *AnAFP* domains in cold resistance of *E. coli*. Two pairs of specific primers (Table S1) with restriction sites of EcoRI/BamHI were designed by using CE Design V1.04 (<http://www.downcc.com/soft/281907.html>), and used to amplify open reading frame (ORF) of *AnAFP* and four mutants deleting domain A (*AnAFP* Δ A), K (*AnAFP* Δ K), S (*AnAFP* Δ S) and N (*AnAFP* Δ N) created in our previous study, respectively. The products were cloned into the EcoRI/BamHI site of prokaryotic expression vector pINIII to generate pIN-

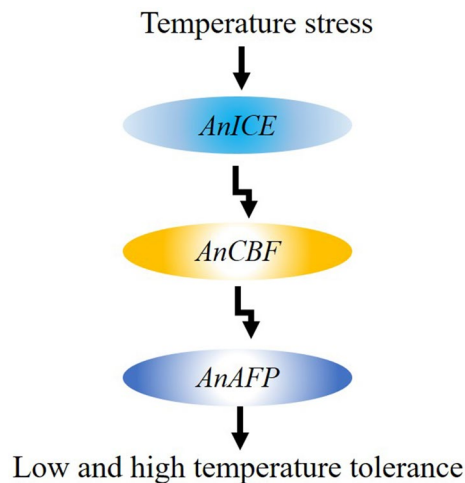


Figure 8. Signaling model of *AnAFP* in *A. nanus* in response to temperature stress.

III-*AnAFP*, pINIII-*AnAFPΔA*, pINIII-*AnAFPΔK*, pINIII-*AnAFPΔS* and pINIII-*AnAFPΔN*, and confirmed by sequencing, respectively.

The re-constructed plasmids were transformed into competent cells of *E. coli* cold-sensitive strain BX04. After confirming by screening with 50 mg/L ampicillin, PCR amplification and sequencing, the positive colonies were transferred into LB liquid medium and incubated at 37 °C until $OD_{600} = 0.5–0.6$. According to the methods of Yang et al.³⁴ and Deng et al.²¹ with minor modification, the cultured cells were treated at 17 °C for 9 days with three replicates. All samples were diluted by 10^0 to 10^7 times, respectively. The 5 μ L and 100 μ L of them were plated onto LB plates with 50 mg/L ampicillin, incubated at 37 °C for 12 h and photographed, respectively. Before treatment, 5 μ L of them were plated onto LB plates with 50 mg/L ampicillin and incubated at 37 °C for 12 h for control. The colonies number with spraying 100 μ L cells were counted and used to calculate average survival rates under cold stress.

Evaluation of *AnAFP* domains in heat resistance of *E. coli*. Two pairs of specific primers (Table S2) with restriction sites of NdeI/HindIII were designed, and used to amplify ORF of *AnAFP*, *AnAFPΔA*, *AnAFPΔK*, *AnAFPΔS* and *AnAFPΔN* using the above plasmids as template, respectively. The products were cloned into Nde I/Hind III site of prokaryotic expression vector pET28a to generate pET28a-*AnAFP*, pET28a-*AnAFPΔA*, pET28a-*AnAFPΔK*, pET28a-*AnAFPΔS* and pET28a-*AnAFPΔN*, and confirmed by sequencing, respectively.

The recombinant plasmids were transferred into competent cells of *E. coli* BL21 (DE3). After confirming by screening with 50 mg/L kanamycin, and PCR amplification and sequencing, the positive colonies were transferred into LB liquid medium and incubated at 37 °C until $OD_{600} = 0.5–0.6$. The ectopic expression of *AnAFP*, *AnAFPΔA*, *AnAFPΔK*, *AnAFPΔS* and *AnAFPΔN* was induced by 0.5 mmol/L IPTG, detected by sodium dodecyl sulfate–polyacrylamide gel electrophoresis (SDS-PAGE). As described by Li et al.³⁵ with minor modification, the induced cells were splinted into six centrifuge tubes, three of them were treated at 50 °C for 30 min, while others were incubated at 37 °C for 30 min, respectively. All samples were diluted by 100 to 104 times, respectively. The 5 μ L and 100 μ L of them were plated onto LB plates with 50 mg/L kanamycin, incubated at 37 °C for 12 h, and photographed. The colonies number with spraying 100 μ L cells were counted and used to calculate average survival rate under heat stress.

Plasmids reconstruction and *Arabidopsis* transformation. Two pairs of specific primers (Table S3) with restriction sites of BspI/PstI were designed, and used to amplify ORF of *AnAFP*, *AnAFPΔA*, *AnAFPΔK*, *AnAFPΔS* and *AnAFPΔN*, respectively. The products were cloned into Bsp I/Pst I site of plants expression vector pCambia2300-35S-*eGFP* to generate 35S-*AnAFP-eGFP*, 35S-*AnAFPΔA-eGFP*, 35S-*AnAFPΔK-eGFP*, 35S-*AnAFPΔS-eGFP* and 35S-*AnAFPΔN-eGFP*, and confirmed by sequencing, respectively. These plasmids were transferred into competent cells of *Agrobacterium tumefaciens* GV3101 by freeze–thaw method.

After confirming by screening with 50 mg/L rifampicin and 50 mg/L kanamycin on YEB plates, PCR amplification and sequencing, the positive colonies were transferred into liquid medium YEB and incubated at 28 °C until $OD_{600} = 1.0–1.5$. The cells were collected by centrifugation at 4 °C and 4000 r/min for 10 min, resuspended and adjusted to $OD_{600} = 1.0$ with 5% (wt/vol) fresh sucrose solution, added surfactant Silwet L-77 to a concentration of 0.02% (vol/vol), and used to transform *Arabidopsis* mutant of the KnS type dehydrin gene *AtH1RD11* (AT1G54410) by floral-dip method.

Heat tolerance of transgenic *Arabidopsis*. As described by Sun et al.³⁶, T_1 seeds were surface-sterilized with 75% ethanol for 1 min and 10% NaClO for 10 min, and plated onto 1/2 MS plates with 50 mg/L kanamycin (Sigma, USA) for screening of transgenic plants, which were used to produce T_2 generation. The T_2 plants with 3:1 segregating-ratio to resistance/susceptibility of kanamycin were self-pollinated to generate T_3 . The homozy-

gous lines without segregation were collected from T₃, and were identified by PCR amplification using the primers (Table S4) for the specific fragments of *AnAFP*, *AnAFPΔA*, *AnAFPΔK*, *AnAFPΔN* and *AnAFPΔS*. The total RNA of every line was extracted by RNA extractor kit (Sangon, China), reacted with RNase-free DNase I, and used to reverse transcribed into cDNA using PrimeScript RT Reagent Kit (TaKaRa, Dalian). The ectopic expression of the transformed genes was identified by reverse transcription PCR (RT-PCR) using the above primers. The *AtActin* gene was amplified and used as reference. Five T₃ lines were planted in pots, and grown in green house at 22 °C and 60–70% relative humidity under a 10 h light/14 h dark photoperiod. One-month-old seedlings were used for heat-shock treatment at 46 °C for 3 h, and recovered for 2 weeks at 22 °C, and investigated for phenotype.

Subcellular localization. The *35S-AnAFP-eGFP*, *35S-AnAFPΔA-eGFP*, *35S-AnAFPΔK-eGFP*, *35S-AnAFPΔS-eGFP* and *35S-AnAFPΔN-eGFP* plasmids were precipitated onto 50 mg of 0.6 μm gold particles by 2.5 mol/L CaCl₂ and 0.1 mol/L spermidine, respectively, and used for transformation of intraepidermal cells of onion bulbs by microprojectile bombardment on DuPont PDS 1000/He (Bio-Rad, USA). The green fluorescence signal was observed using laser confocal microscope LSM 800 (Carl Zeiss, Germany).

Yeast two-hybrid. Two pairs of specific primers (Table S5) with restriction sites of NdeI/BamHI were designed, and used to amplify ORF of *AnAFP*, *AnAFPΔA*, *AnAFPΔK*, *AnAFPΔS* and *AnAFPΔN*, respectively. The products were cloned into NdeI/BamHI sites of yeast two hybrid (Y2H) bait vector pGBKT7 to generate pGBKT7-*AnAFP*, pGBKT7-*AnAFPΔA*, pGBKT7-*AnAFPΔK*, pGBKT7-*AnAFPΔS* and pGBKT7-*AnAFPΔN*, and confirmed by sequencing, respectively. Another pair of specific primers (Table S6) with restriction sites of NdeI/BamHI were designed and used to amplify ORF of *AnICE1* from the cDNA of *A. nanus* seedlings. The products were cloned into Y2H trap vector pGADT7 to generate pGADT7-*AnICE1* and confirmed by sequencing.

The yeast strain Y2H Gold was transformed with every plasmid using Yeastmaker Yeast Transformation System 2 (Clontech, Japan), and used to test of self-activation and toxicity of *AnAFP*, *AnAFPΔA*, *AnAFPΔK*, *AnAFPΔN*, *AnAFPΔS*, and *AnICE1* proteins. Subsequently, the yeast strain Y2H Gold was co-transformed by each pair of bait vector pGBKT7-*AnAFP*, pGBKT7-*AnAFPΔA*, pGBKT7-*AnAFPΔK*, pGBKT7-*AnAFPΔN*, pGBKT7-*AnAFPΔS*, and trap vector pGADT7-*AnICE1*, respectively. The transformants were screened on the auxotroph SD/-Trp-Leu plates at 30 °C for 3–5 days. The mono-colonies were transferred onto the auxotroph SD/-Leu-Trp-His-Ade plates, incubated at 30 °C for 3–5 days, and strained with X-α-Gal.

Real-time quantitative PCR. The seeds of *A. nanus* were surface-sterilized with 75% ethanol for 10 min, and planted in soil and grown in green house at 25 °C 12 h light/ 20 °C 12 h dark and 60–70% relative humidity. At the six-leaf stage, the seedlings with same size were treated at high temperature of 45 °C for 0 (negative control), 3, 6, 12, and 24 h with three biological replicates, as described by Yu et al.³⁷. The total RNA was extracted, and reverse transcribed into cDNA as above.

For pairs of specific primers (Table S7) were designed, and used to amplify a 150–250 bp fragment for *AnAFP*, *AnAFPΔA*, *AnAFPΔK*, *AnAFPΔN* and *AnAFPΔS*, as well as the internal reference gene *AnGAPDH*. The RT-qPCR was performed using SYBR Green Super Mix (Bio-Rad, USA) by two step real-time PCR cycles (95 °C 30 s; 95 °C 5 s, 50–65 °C 30 s, 39 cycles) in CFX96 Real-Time System (Bio-Rad, USA). The 2^{-ΔΔCT} method was used to normalize the expression differentiation between reference gene and investigated genes³⁸.

Statistical analysis. All experiments were conducted with three replicates. The data are presented as the mean values ± standard deviation (SD). Statistical difference was analyzed using Student's t tests.

Received: 6 January 2021; Accepted: 7 April 2021

Published online: 19 April 2021

References

- Guy, C. L. Freezing tolerance of plants: Current understanding and selected emerging concepts. *Can. J. Bot.* **81**, 1216–1223 (2003).
- Hong, J. H. et al. A sacrifice-for-survival mechanism protects root stem cell niche from chilling stress. *Cell* **170**, 102–113 (2017).
- Berlett, B. S. & Stadtman, E. R. Protein oxidation in aging, disease, and oxidative stress. *J. Biol. Chem.* **272**, 20313–20316 (1997).
- Farmer, E. E. & Mueller, M. J. ROS-mediated lipid peroxidation and RES-activated signaling. *Ann. Rev. Plant Biol.* **1**, 429–450 (2013).
- Zhu, J. K. Abiotic stress signaling and responses in plants. *Cell* **167**, 313–324 (2016).
- Ding, Y., Shi, Y. & Yang, S. Advances and challenges in uncovering cold tolerance regulatory mechanisms in plants. *New Phytol.* **222**, 1690–1704 (2019).
- Ma, Y., Dai, X. Y. & Xu, Y. Y. COLD1 confers chilling tolerance in rice. *Cell* **160**, 1209–1221 (2015).
- Wang, W. H., He, E. M., Guo, Y., Tong, Q. & Zheng, H. Chloroplast calcium and ROS signaling networks potentially facilitate the primed state for stomatal closure under multiple stresses. *Environ. Exp. Bot.* **122**, 85–93 (2016).
- Stockinger, E. J., Gilmour, S. J. & Thomashow, M. F. *Arabidopsis thaliana* CBF1 encodes an AP2 domain-containing transcriptional activator that binds to the C-repeat/DRE, a cis-acting DNA regulatory element that stimulates transcription in response to low temperature and water deficit. *Proc. Nat. Acad. Sci. USA* **94**, 1035–1040 (1997).
- Chinnusamy, V., Ohta, M. & Kanrar, S. ICE1: A regulator of cold-induced transcriptome and freezing tolerance in *Arabidopsis*. *Gene. Dev.* **17**, 1043–1054 (2003).
- Baena-Gonzalez, E. & Sheen, J. Convergent energy and stress signaling. *Trends Plant Sci.* **13**, 474–482 (2008).
- Cheung, R. C. F., Ng, T. B. & Wong, J. H. Antifreeze proteins from diverse organisms and their applications: An overview. *Curr. Protein. Pept. Sc.* **18**, 262–283 (2017).

13. Hightower, R., Baden, C., Penzes, E., Lund, P. & Dunsmuir, P. Expression of antifreeze proteins in transgenic plants. *Plant. Mol. Biol.* **17**, 1013–1021 (1991).
14. Khanna, H. K. & Daggard, G. E. Targeted expression of redesigned and codon optimized synthetic gene leads to recrystallisation inhibition and reduced electrolyte leakage in spring wheat at subzero temperatures. *Plant. Cell. Rep.* **25**, 1336–1346 (2006).
15. Wang, Y. *et al.* Expression of insect (*Microdera punctipennis dzungarica*) antifreeze protein MpAFP149 confers the cold tolerance to transgenic tobacco. *Plant Cell Rep.* **27**, 1349–1358 (2008).
16. Griffith, M. & Yaish, M. W. F. Antifreeze proteins in overwintering plants: A tale of two activities. *Trends Plant Sci.* **9**, 399–405 (2004).
17. Bredow, M., Vanderbeld, B. & Walker, V. K. Ice-binding proteins confer freezing tolerance in transgenic *Arabidopsis thaliana*. *Plant. Biotechnol. J.* **15**, 68–81 (2017).
18. Pudney, P. D., Buckley, S. L. & Sidebottom, C. M. The physicochemical characterization of a boiling stable antifreeze protein from a perennial grass (*Lolium perenne*). *Arch. Biochem. Biophys.* **410**, 238–245 (2003).
19. Kuiper, M. J., Davies, P. L. & Walker, V. K. A theoretical model of a plant antifreeze protein from *Lolium perenne*. *Biophys. J.* **81**, 3560–3565 (2001).
20. Yu, S., Yin, L. & Mu, S. Discovery of an antifreeze protein in the leaves of *Ammopiptanthus nanus*. *Can. J. Plant Sci.* **90**, 35–40 (2010).
21. Deng, L. Q. *et al.* Heterologous expression of antifreeze protein gene *AnAFP* from *Ammopiptanthus nanus* enhances cold tolerance in *Escherichia coli* and tobacco. *Gene* **539**, 132–140 (2014).
22. Zhang, Y. *et al.* Chilling tolerance identification of transgenic maize with antifreeze protein gene (*AnAFP*) of *Ammopiptanthus nanus* and chilling tolerance mechanism. *Crop J.* <https://doi.org/10.1016/j.cj.2020.08.011> (2020).
23. Koag, M. *et al.* The K-segment of maize DHN1 mediates binding to anionic phospholipid vesicles and concomitant structural changes. *Plant Physiol.* **150**, 1503–1514 (2009).
24. Daley, M. E. & Sykes, B. D. The role of side chain conformational flexibility in surface recognition by *Tenebrio molitor* antifreeze protein. *Protein Sci.* **12**, 1323–1331 (2003).
25. Maya, B. D., Ido, B. & Peter, L. D. Ice-binding proteins and their function. *Ann. Rev. Biochem.* **85**, 515–542 (2016).
26. Liu, Y., Wang, L., Zhang, T., Yang, X. & Li, D. Functional characterization of KS-type dehydrin ZmDHN13 and its related conserved domains under oxidative stress. *Sci. Rep.* **7**, 7361 (2017).
27. Chakrabortee, S. *et al.* Intrinsically disordered proteins as molecular shields. *Mole. Biosyst.* **8**, 210–219 (2012).
28. Stephanie, L. H. *et al.* The importance of size and disorder in the cryoprotective effects of dehydrins. *Plant Physiol.* **163**, 1376–1386 (2013).
29. Lissarre, M., Ohta, M., Sato, A. & Miura, K. Cold-responsive gene regulation during cold acclimation in plants. *Plant. Signal Behav.* **5**, 948–952 (2010).
30. Vazquez-Hernandez, M., Romero, I., Escibano, M. I., Merodio, C. & Sanchez-Ballesta, M. T. Deciphering the role of CBF/DREB transcription factors and dehydrins in maintaining the quality of table grapes cv. autumn royal treated with high CO₂ levels and stored at 0 °C. *Front. Plant Sci.* **8**, 1591 (2017).
31. Jaglo-Ottosen, K. R., Gilmour, S. J., Zarka, D. G., Schabenberger, O. & Thomashow, M. F. *Arabidopsis CBF1* overexpression induces *COR* genes and enhances freezing tolerance. *Science* **280**, 104–106 (1998).
32. Gilmour, S. J., Fowler, S. G. & Thomashow, M. F. *Arabidopsis* transcriptional activators *CBF1*, *CBF2*, and *CBF3* have matching functional activities. *Plant Mol. Biol.* **54**, 767–781 (2004).
33. Swindell, W. R., Huebner, M. & Weber, A. P. Transcriptional profiling of *Arabidopsis* heat shock proteins and transcription factors reveals extensive overlap between heat and non-heat stress response pathways. *BMC Genomics* **8**, 125 (2007).
34. Yang, C. *et al.* A novel cold-regulated cold shock domain containing protein from scallop *Chlamys farreri* with nucleic acid-binding activity. *PLoS ONE* **7**, e32012 (2012).
35. Li, D., Yang, F., Lu, B., Chen, D. & Yang, W. Thermotolerance and molecular chaperone function of the small heat shock protein HSP20 from hyperthermophilic archaeon, *Sulfolobus solfataricus* P2. *Cell Stress Chaperone* **17**, 103–108 (2012).
36. Sun, F. A. *et al.* Maize ZmBES1/BZR1-5 decreases ABA sensitivity and confers tolerance to osmotic stress in transgenic *Arabidopsis*. *Int. J. Mol. Sci.* **21**, 996 (2020).
37. Yu, H. *et al.* Cloning and characterization of vacuolar H⁺-pyrophosphatase gene (*AnVP1*) from *Ammopiptanthus nanus* and its heterologous expression enhances osmotic tolerance in yeast and *Arabidopsis thaliana*. *Plant Growth Regul.* **81**, 385–397 (2017).
38. Livak, K. J. & Schmittgen, T. D. Analysis of relative gene expression data using real-time quantitative PCR and the 2^{-ΔΔCT} method. *Methods* **25**, 402–408 (2001).

Acknowledgements

This research was funded by the National Key Science and Technology Special Project (2016ZX08003004-005), and the Applied Basic Project of Science and Technology Department of Sichuan Province (2018JY0470). We thank Professor Wei Chi from Institute of Botany, Chinese Academy of Sciences for presenting the pINIII vector and *E. coli* BX04 strain. The present study complies with all relevant institutional, national, and international guidelines and legislation.

Author contributions

H.Y. administrated the project. H.Z. carried out the experiments. Y.Z. analyzed the data. H.Y. and W.L. wrote the manuscript. Y.L., and Q.Y. took part in the experiments. F.F. provided technical support. Y.Z. and F.F. designed the research. All the authors approved the final manuscript.

Competing interests

The authors declare no competing interests.

Additional information

Supplementary Information The online version contains supplementary material available at <https://doi.org/10.1038/s41598-021-88021-0>.

Correspondence and requests for materials should be addressed to Y.Z. or F.F.

Reprints and permissions information is available at www.nature.com/reprints.

Publisher's note Springer Nature remains neutral with regard to jurisdictional claims in published maps and institutional affiliations.



Open Access This article is licensed under a Creative Commons Attribution 4.0 International License, which permits use, sharing, adaptation, distribution and reproduction in any medium or format, as long as you give appropriate credit to the original author(s) and the source, provide a link to the Creative Commons licence, and indicate if changes were made. The images or other third party material in this article are included in the article's Creative Commons licence, unless indicated otherwise in a credit line to the material. If material is not included in the article's Creative Commons licence and your intended use is not permitted by statutory regulation or exceeds the permitted use, you will need to obtain permission directly from the copyright holder. To view a copy of this licence, visit <http://creativecommons.org/licenses/by/4.0/>.

© The Author(s) 2021